

# A microstructural and corrosion resistance study of (Zr, Si, Ti)N-Ni coatings produced through co-sputtering

Estrella Natali Borja-Goyeneche & Jhon Jairo Olaya-Florez

*Departamento de Ingeniería Mecánica y Mecatrónica, Facultad de Ingeniería, Universidad Nacional de Colombia, Bogotá, Colombia.  
enborjag@unal.edu.co, jjolayaf@unal.edu.co*

Received: July 19<sup>th</sup>, 2018. Received in revised form: October 4<sup>th</sup>, 2018. Accepted: October 24<sup>th</sup>, 2018.

## Abstract

This work researches the influence of the nickel content on the structural and anticorrosive properties of ZrSiTiN films deposited by means of reactive co-sputtering on alloys of Ti6Al4V. The morphology and structure were analyzed by means of scanning electron microscopy (SEM) and X-ray diffraction (XRD), and the chemical composition was identified via X-ray scattering spectroscopy (EDS). The corrosion resistance was studied using potentiodynamic polarization (PP) tests employing a 3.5% by weight NaCl solution. In the films, an increase of Ni up to 6.97 at% was observed, while in XRD the FCC phase of (Zr, Ti) N was identified, with a mixed orientation in planes (111) and (200), which tended to diminish with the increase of Ni. Finally, with the addition of Ni, the corrosion current densities were reduced from  $5.56 \times 10^{-8}$  to  $2.64 \times 10^{-9} A/cm^2$ . The improvement in the corrosion resistance is due to the effect of the Ni on the microstructure of the system (Zr, Ti) N, which can improve the quality of the passive film and prevent crystalline defects and corrosion zones.

*Keywords:* sputtering; thin films; corrosive; nickel.

# Un estudio de la microestructura y resistencia a la corrosión de recubrimientos de (Zr, Si, Ti)N-Ni producidas mediante co-sputtering

## Resumen

En el presente trabajo se investiga la influencia del contenido de níquel sobre las propiedades estructurales y anticorrosivas de películas de TiSiZrN depositadas mediante co-sputtering reactivo sobre aleaciones de Ti6Al4V. La morfología y estructura se realizó mediante microscopía electrónica de barrido (SEM) y difracción de rayos X (XRD), y la composición química se identificó mediante espectroscopía de dispersión de rayos X (EDS). La resistencia a la corrosión se estudió mediante ensayos de polarización potenciodinámica (PP) utilizando una solución de NaCl al 3.5% en peso. En las películas se observó un aumento del Ni hasta 6,97 at%, mientras que en XRD se identificó la fase fcc de (Zr,Ti)N, con una orientación mixta en los planos (111) y (200), la cual tiende a reducir con el incremento de Ni. Finalmente, con la adición de Ni se redujeron las densidades de corriente de corrosión de  $5,56 \times 10^{-8}$  a  $2,64 \times 10^{-9} A/cm^2$ . La mejora de la resistencia a la corrosión se debe efecto del Ni sobre la microestructura del sistema (Zr, Ti)N, las cuales pueden mejorar la calidad de la película pasiva, prevenir defectos cristalinos y zonas de corrosión.

*Palabras clave:* sputtering; películas delgadas; corrosión; níquel.

## 1. Introduction

Super-hard nanostructured metallic nitride coatings have improved the service life and the maintenance cycle of cutting tools, aeronautical parts, and automobiles. The latest

advances in the development of new materials and techniques for producing thin films have focused on the use of hard and wear-resistant applications. These results have been very well received thanks to the efforts to increase the duration of materials in the diamond range. These coatings are divided

**How to cite:** Borja-Goyeneche, E.N. and Olaya-Florez, J.J. A microstructural and corrosion resistance study of (Zr, Si, Ti)N-Ni coatings produced through co-sputtering DYNA, 85(207), pp. 192-197, Octubre - Diciembre, 2018.

into two groups, depending on the hardness value. The first is called hard coatings, which have a hardness of  $>12$  GPa, and the second super-hard coatings, which have a hardness of  $>40$  GPa. Currently, significant efforts are devoted to improving the formation of nanocomposite coatings using magnetron sputtering, since this technology can be easily extended for industrial use [1].

Titanium nitride (TiN) coating has wide applications in the fields of space, biomedicine, and microelectronics, given its excellent physical, chemical, electrical, and mechanical properties. The properties that allow titanium nitride to be applicable in so many fields are its high hardness, good adhesive wear, high resistance to corrosion, high melting temperature, and biocompatibility. However, one of the most significant developments in hard coatings has been the synthesis of the Ti-Si-N system, with hardness values above 40 GPa [2,3]. These improved properties of the Ti-Si-N system are attributed to the formation of transition metal nitride nanocrystals embedded in an amorphous matrix of a second phase of the material [4]. The above can be explained by the mechanism of spinodal decomposition, through which an alloy is decomposed into equilibrium phases. This is a medium for the rapid separation of a mixture of liquids or solids from a thermodynamic phase to form two coexisting phases. For the Ti-Si-N system, there is an amorphous phase of SiN and TiN nanocrystals.

Zirconium nitride (ZrN) coatings are used as diffusion barriers in microelectronics, wear-resistant coatings in cutting tools, or as corrosion-resistant layers in mechanical and optical components [5], and furthermore they show high hardness and low electrical resistivity. The incorporation of silicon in coatings, such as in the Zr-Si-N system, increases the films' hardness, improves the oxidation resistance of the films, and reduces the friction coefficient [6]. Hasong Choi et al. [5] mention that the addition of silicon from 0 to 5.8 at% into the ZrN columnar coating transforms it into a nanocomposite structure composed of ZrN nanocrystals that are embedded in the amorphous matrix of Si<sub>3</sub>N<sub>4</sub>; if a higher silicon percentage is added, amorphous coatings can be produced [4].

However, the quaternary system of ZrSiTiN has not been thoroughly studied. Nevertheless, there are references that show the behavior of the coating and its characteristic properties of hardness, oxidation resistance, and structure. This coating has been deposited using various techniques, such as high-frequency arc evaporation (HF) and the co-sputtering technique. The presence of alloying elements such as Zr contributes to better wear resistance, while Si increases hardness and thermal stability [7]. Pogrebniak et al. [7] determined that the nanograin size of the solution changed from 10 nm to 12 nm, and at the same time the size of the intermediate layer of  $\alpha - Si_3N_4$  that enveloped the nanograins of (Ti,Zr)N varied from 6 nm to 8 nm, while the hardness varied from 39.6 GPa to 53.6 GPa [7]. On the other hand, I. A. Saladukhin et al. [8] found that the increase in hardness in the ZrSiTiN thin film is due to the formation of SiN, which has the function of hindering the growth of the transition metal nitride grains, which entails a refinement of grain size [8]. However, an additional increase in silicon can reduce the hardness, which is attributed to the progressive

thickening of the amorphous interfacial phase of Si<sub>3</sub>N<sub>4</sub> and the concurrent decrease in size and amorphization of the solid solution grains [9,10].

In recent years, hard coating properties have been improved by the addition of nickel. For example, Chu et al. [11] show that the addition of Ni to TiN improves the hardness by approximately 60% over the values of the mixing rule. A value of  $3,200 \text{ kgf/mm}^2$  was reported for a layer thickness ratio over the period ( $l_{Ni}/\Lambda$ ) of  $l_{Ni}/\Lambda = 0.3$ . Zhang et al. [12] demonstrate that for films with 2.1% Ni, a maximum temperature of 850°C was determined, below which an excellent resistance to oxidation prevails, but above which oxidation takes place at an exponential rate, accompanied by a sudden increase in surface roughness. Likewise, nickel does not participate in the oxidation process within the temperature range studied but rather exists in a metallic state. Suna et al. [9] researched into the microstructure of Zr-Ni-N films with low nickel content deposited by reactive sputtering; the findings show that due to the columnar microstructure, the grain size, and the shape of the crystallites, the hardness improves to 32 GPa and the residual stresses are compression, with values of -2GPa. Yet the addition of nickel favors Zr-Ni-N films with normal nanocolumns to the substrate, thus obtaining a columnar structure that improves the hardness and residual compression effects [9]. Likewise, the FCC (Zr, Ti)N phase oriented in the planes (111) and (200), the amorphous or crystalline Si<sub>3</sub>N<sub>4</sub> compound oriented in the planes (201), (210), and (202), and ZrN in planes (111), (200), and (311) have been found via XRD [7].

The objective of this paper is to research into the structure and anticorrosive properties of the system composed of Zr-Si-Ti-N with different Ni contents, deposited on Ti6Al4V substrates via the co-sputtering technique. This material was characterized by means of SEM, EDS, and X-ray diffraction, and the electrochemical behavior was studied through potentiodynamic polarization curves to determine the corrosion current density.

## 2. Experimental procedure

### 2.1. Deposition and coating growth

Zr-Si-Ti-N coating with added nickel was deposited via the co-sputtering technique in a combined atmosphere of nitrogen-argon on silicon wafer, glass, and Ti6Al4V alloy. The sputtering equipment has two magnetrons of 4-inch targets, each inside a vacuum chamber. The system can generate the vacuum with a rotary vane mechanical pump and a turbomolecular pump with a pumping speed of  $10 \text{ m}^3/\text{h}$  and  $1,800 \text{ m}^3/\text{h}$ , respectively. The co-sputtering system has an arrangement with two magnetrons in a confocal configuration locating the targets at 30° with respect to the normal of the target surface and a working distance of 10.16 cm (4 in). During the coating's growth, the substrates were rotating at 10 rpm, with the aim of achieving better homogenization of the nickel in the coating.

The procedure used targets of a transition metal or an alloy composed of two transition metals, which have commercial composition with a purity of 99.9% and a diameter of 10cm. To

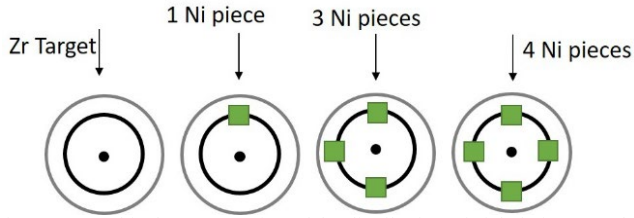


Figure 1. Graphical representation of the distribution of nickel pieces on the zirconium target.  
Source: The authors.

generate the discharge, a Zr target was used connected to a pulsed-DC source with a power of 200 W and a target of Ti<sub>5</sub>Si<sub>2</sub> connected to an RF source with a power of 170 W. Argon and nitrogen were introduced with fluxes of 14 sccm and 2 sccm, respectively. The working pressure was 4x10<sup>-3</sup> mbar, and the base pressure of the chamber was below 9x10<sup>-6</sup> mbar. The deposit time of the films was 80 minutes.

The coating’s production was carried out while varying the amount of 99.99% high purity nickel metal squares to cover the area of greatest erosion of the Zr target, also known as the “race track.” Fig. 1 shows a diagram of the distribution of Ni pieces of 3x3x3 mm on the target of Zr.

### 2.2. Characterization of the coatings

A Bruker GT optical profilometer was used to measure the thickness, taking 3 measurements per test piece. The measurement was made on silicon that had a laminar shape and allowed the measurement to be optimal. The structural characterization was performed by X-ray diffraction with Panalytical X-PerTPro equipment in Bragg-Brentano mode and a ground beam. The measurements were made with a monochromatic line K of copper, wavelength 1.54 Å, current intensity 40 mA, and radiation source 45 kV. The sweep range was within the range of 10° to 100°, with a step size of 0.02° in continuous mode. From the Williamson-Hall method and the Debye Scherrer equation [9].

$$\beta_t^2 = (\beta_c)^2 + (\beta_m)^2 + C^2 \tag{1}$$

The crystallite size and the microdeformation were determined, using a non-linear adjustment with the Pseudo-Voight function through Origin pro9.0 software.

$$y = (A / \cos(x))^2 + (B * \tan(x))^2 + C \tag{2}$$

The surface morphology of the coating was determined by scanning electron microscopy (SEM) using a FEI QUANTA 200 scanning electron microscope. Images of backscattered X-ray electrons (BSI) and BSI point map images were obtained from the surface of the films to characterize the surfaces or areas of corrosion that were produced in the electrochemical tests. The chemical composition was evaluated with an EDS detector coupled to

a microscope in order to determine the chemical composition at different points of the sample. The usual conditions under which the equipment is operated are the same as for SEM, but the potential difference is higher, since it is required to generate the X-ray emissions that are characteristic of the elements present in the coating.

The corrosion resistance of the ZrSiTiN+Ni coatings was studied using a three-electrode system in a Gamry 600 potentiostat at room temperature. The samples were mounted in a special cell, in which the exposed area was 0.196 cm<sup>2</sup>. In the corrosion resistance experiments, the substrates were used as a working electrode with a platinum one as the counter electrode, and a 3.5% NaCl solution was used as the electrolyte (pH 7.9). Before performing each experiment, the corrosion potential was allowed to stabilize for 45 minutes of immersion in the solution. In the potentiodynamic polarization conduction (PP) experiments, the initial potential was -0.3V and the scanning speed was 0.5 mV/s. The corrosion current density (I<sub>corr</sub>) was estimated by a linear adjustment using extrapolation by Tafel in the Gamry Echem Analyst Software.

### 3. Results and discussion

Table 1 shows the semiquantitative analysis of the coatings produced as a function of the number of Ni pellets added to the Zr target. It can also be seen that the coatings have high contents of Zr, attributed to the high current density applied to the Zr target. However, it can be seen that as the Ni percentage increases, the Zr decreases. The percentage of nickel increases up to 6.9% as Ni is added to the Zr target, and the Zr percentage decreases from 72.05 to 58.21 at%, while the Si and Ti contents do not vary significantly.

Fig. 2 shows the results for deposit rates in the produced coatings. It can be seen that the coatings deposited without nickel showed the highest values of thickness, 1.31 μm ± 0.15 μm, while the addition of nickel reduced the films’ thickness, with values of 1.14 μm ± 0.13 μm (3.34 at% Ni), 1.069 μm ± 0.12 μm (6.05 at% Ni), and 1.133 μm ± 0.13 μm (6.97 at% Ni). It is possible that the nickel in the erosion zone of the Zr target produces a decrease in the polarization of the target due to the lower emission of secondary electrons; that is, the efficiency of the sputtering decreases.

Fig. 3 shows how the discharge current for the Zr target decreases with the addition of Ni. There is definitely a lower emission of electrons from the plasma at the target surface, i.e., a decrease in the ionization of the plasma and a reduction of sputtering efficiency.

Table 1. Chemical composition for Ti6Al4V alloy depending on the nickel addition.

Nickel cubes	Zr	Std Dev	Si	Std Dev	Ti	Std Dev	Ni	Std Dev
0	69.27	0.2	11.6	0.3	18.01	0.2	0	0
1	64.64	0.4	13.17	0.9	18.87	0.3	3.34	0.9
2	58.68	0.6	11.77	1	17.81	0.2	4.34	0.8
3	60.54	0.3	12.24	0.5	18.31	1	6.05	0.7
4	58.21	0.6	12.61	0.8	19.34	0.4	6.97	0.3

Source: The authors.

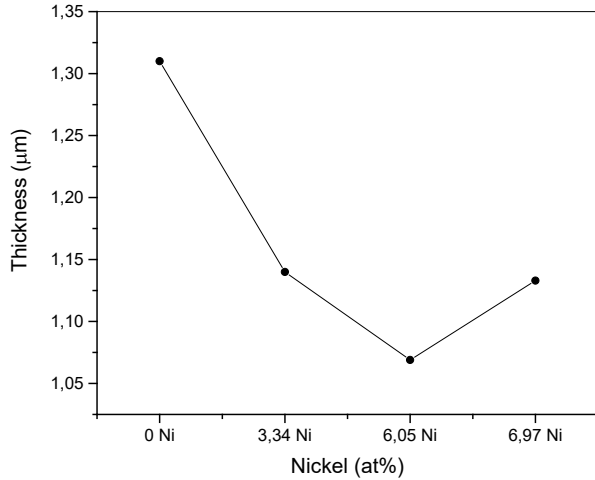


Figure 2. Film thickness depending on the percentage of nickel. Source: The authors.

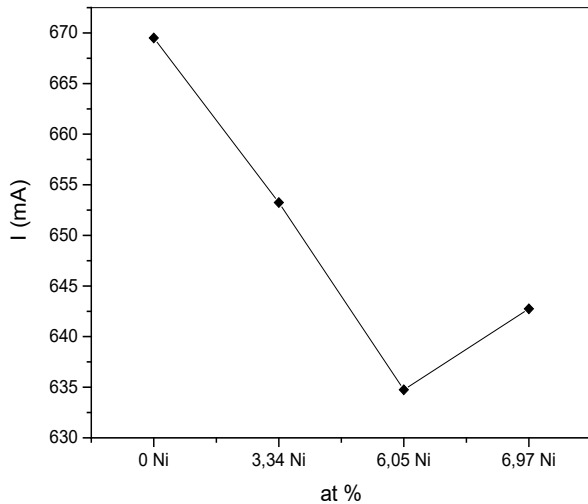


Figure 3. Current behavior as a function of nickel addition. Source: The authors.

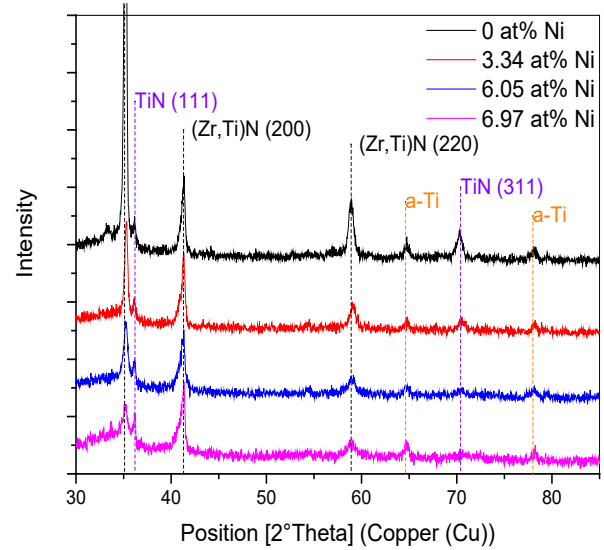


Figure 4. X-ray diffraction pattern of thin film ZrSiTiNi. Source: The authors.

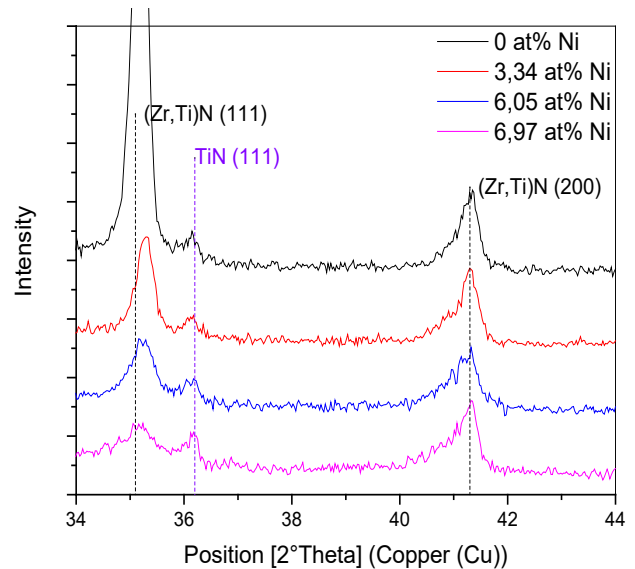


Figure 5. X-ray diffraction pattern of ZrSiTiN with different nickel content. Source: The authors.

Fig. 4 shows the X-ray diffraction results in the coatings produced as a function of the Ni content, and Fig. 5 shows the  $2\theta = 34-44^\circ$  interval of the XRD pattern, in order to better observe the most important signals found in the material. In general, it is possible to see the presence of the related peaks of the substrate and the signals of the FCC (Zr, Ti)N phase in the planes (111) and (200) and the TiN in the plane (311) with cubic structure. These results correspond with the works of Pogrebnjak [7] and Sobol [13], who explained their results by a substitution mechanism in solid solution of Ti and Zr atoms when they deposited TiZrN and TiZrSiN coatings.

A decrease in the intensity of the peaks can also be observed as the percentage of nickel increases; that is, the addition of nickel favors the formation of an amorphous material. In these coatings, the formation of amorphous regions due to the low deposition temperature is favored. For example, the  $\text{Si}_3\text{N}_4$  produced by sputtering is amorphous, because the temperature for the formation of  $\text{Si}_3\text{N}_4$  crystals is

higher than  $800^\circ\text{C}$  [14,15]. It was also found that Ni can be incorporated in a crystalline form in a solid solution when the substrate temperature is higher than  $600^\circ\text{C}$  [15]. The low temperatures and the amount of nickel definitely reduce the mobility of the absorbed atoms, avoiding the diffusion of the atoms and their occupation of places of minimum energy or the formation of an ordered material.

The results of the crystallite size (D) and microdeformations ( $\epsilon$ ) are shown in Fig. 6. It can be seen that coatings without Ni have the largest crystallite size, and that the crystallite size of the coating decreases as nickel is added. The average crystallite size estimated by the Scherrer equation (Eq. 1) is between 53.43 nm and 16.69 nm. The effect of reducing or refining the crystallite size can be associated with the presence of a small amount of metallic Ni

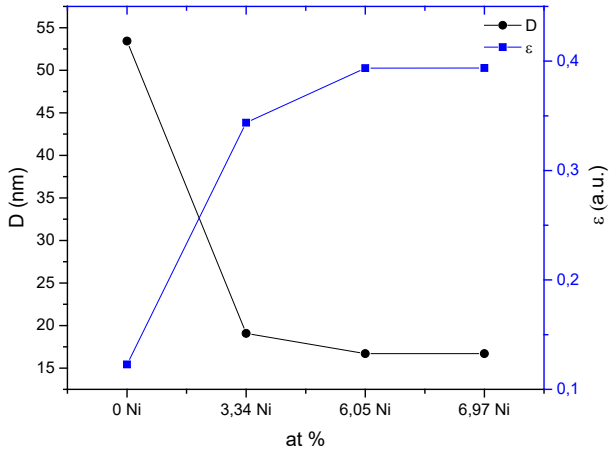


Figure 6. Crystallite size (D) for the (Zr,Ti)N phase and microdeformations ( $\epsilon$ ) depending on the nickel addition. Source: The authors.

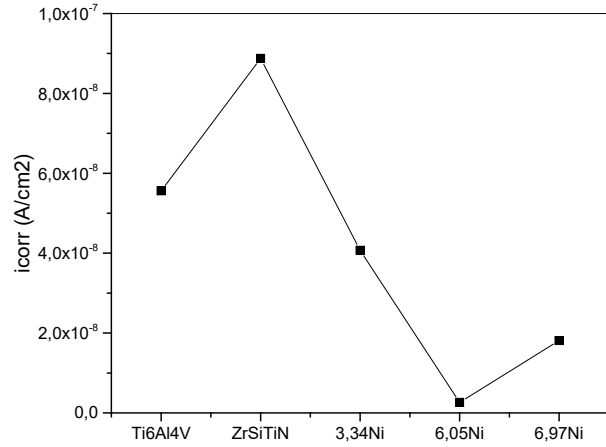


Figure 8. Corrosion density curve based on the nickel addition for the Ti6Al4V alloy. Source: The authors.

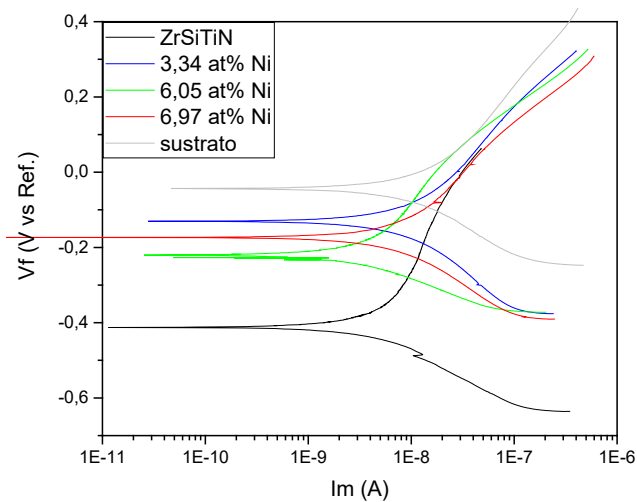


Figure 7. Comparative potentiodynamic polarization curves of the ZrSiTiN coating with addition of nickel on the Ti6Al4V substrate. Source: The authors.

in addition to the Ni dissolved in the (Zr, Ti) N lattice. In the TiN coating with Ni, a decrease in the grain size was found to be the result of the crystallization of the metallic Ni. In addition, the presence of nickel in the thin film is probably found in isolation, but it is not creating solutions of SiNi or TiNi, due to the low diffusion between the atoms of Ni with Si, N, or Ti at room temperature by sputtering [16]. The results of this research also show an increase in the microdeformation of the coatings with the increase of nickel. This may be associated with the amorphous regions restricting the growth of crystallites in the material, generating an increase in residual stresses [16].

Fig. 7 shows the results of the potentiodynamic polarization test on the Ti6Al4V alloy, as well as the results of the ZrSiTiN coatings based on the Ni content. The results of the test carried out on the alloy show a corrosion potential value of  $-4.39E^{-2}V$  and a corrosion current density of  $1.86E^{-8} A$ . Nonetheless, when comparing the potential of

corrosion of the substrate, it is possible to observe a slightly more positive value than that of the deposited coatings, and on the horizontal axis the polarization curves exhibit a shift to the left, which means a lower corrosion density with respect to the alloy.

Fig. 8 shows the change in the corrosion current density of the ZrSiTiN thin films with the addition of nickel on the Ti6Al4V substrate. The thin film that has the best corrosion resistance for the lowest corrosion density is the film with 6.05 at% Ni. When the coating has 6.97 at% Ni, the corrosion resistance increases in relation to the value of the thin film with 6.05 at% Ni; this indicates that up to a certain percentage of added nickel, the coating has greater resistance to corrosion. In general, the corrosion current has lower values each time the nickel increases, and the corrosion potential varies depending on the amount of nickel in each film.

Nickel, a metallic material and a natural resource, proves to be a versatile element and highly resistant to corrosion and high temperatures. It also can be alloyed with many metals. The increased production of nickel is used to improve the mechanical properties of stainless steels, and these steels are used in the aeronautical, automotive, naval, and biomedical industries. According to some research on the microstructures of the compounds of Ti-Zr-Si-N, several factors can illustrate the improvement of the resistance to corrosion [17,18]. This improvement in the resistance to corrosion can be attributed in part to the combination of Ni, Si<sub>3</sub>N<sub>4</sub>, and the phase of (Zr, Ti) N. At the same time, nickel is a corrosion inhibitor and in thin films favors the formation of an amorphous material, which reduces the paths or crystalline defects so that the corrosive solution does not reach the substrate. Furthermore, it is also possible that the Ni embedded in the phase (Zr, Ti) N can help prevent the growth of corrosive regions, and the incorporation of oxides of Si, Ti and Zr that can accelerate the process of passivation of the material [17].

#### 4. Conclusions

Coatings of (ZrSiTi)N with added nickel were produced up to 6.9 at%. As Ni was added to the Zr target, the Zr percentage decreased from 72.05 to 58.21 at%. However, the silicon and titanium contents did not vary significantly in the films produced.

In general, the presence of the related peaks of the substrate and the signals of the FCC phase of (Zr, Ti) N in planes (111) and (200) can be seen. A decrease in intensity of the peaks can also be observed as the percentage of nickel increases; i.e., the addition of nickel favors the formation of an amorphous material. When nickel is added, the crystallite size of the coating decreases. The average crystallite size estimated by the Scherrer equation is between 53.43 nm and 16.69 nm. The results of this research also show an increase in the microdeformation of the coatings with the increase in nickel.

In general, the corrosion current density in the deposited coating takes lower values with an increase in nickel. The Ni inhibits corrosion and promotes the growth of a less crystalline material; that is, it reduces the paths or crystalline defects so that the solution cannot chemically interact with the substrate, thus delaying the degradation of the coating-substrate system.

#### Acknowledgements

Estrella Borja appreciates the financial support received to carry out this research by the National Call for Young Researchers and Innovators 2016 of Colciencias. This research was funded by Universidad Nacional Colombia through project 37935.

#### Bibliography

- [1] Wasa, K., Kanno, I. and Kotera, H., Handbook of sputter deposition technology: Fundamentals and applications for functional thin films, nanomaterials, and MEMS, Second Edi., Elsevier B.V., 2012.
- [2] Vepřek, S., Reiprich, S. and Shizhi, L., Superhard nanocrystalline composite materials: The TiN/Si 3 N 4 system. Appl. Phys. Lett., 66(20), pp. 2640-2642, 1995. DOI: 10.1063/1.113110.
- [3] Zhang, R.F. and Veprek, S., On the spinodal nature of the phase segregation and formation of stable nanostructure in the Ti – Si – N system. 424, pp. 128-137, 2006. DOI: 10.1016/j.msea.2006.03.017.
- [4] Martin, P.J., Bendavid, A., Cairney, J.M. and Hoffman, M., Nanocomposite Ti-Si-N, Zr-Si-N, Ti-Al-Si-N, Ti-Al-V-Si-N thin film coatings deposited by vacuum arc deposition. Surf. Coatings Technol., 200(7), pp. 2228-2235, 2005. DOI: 10.1016/j.surfcoat.2004.06.012
- [5] Choi, H., Jang, J., Zhang, T., Kim, J.H., Park, I.W. and Kim, K.H., Effect of Si addition on the microstructure, mechanical properties and tribological properties of Zr-Si-N nanocomposite coatings deposited by a hybrid coating system. Surf. Coatings Technol., 259(PC), pp. 707-713, 2014. DOI: 10.1016/j.surfcoat.2014.10.008.
- [6] Pilloud, D., Pierson, J.F. and Pichon, L., Influence of the silicon concentration on the optical and electrical properties of reactively sputtered Zr-Si-N nanocomposite coatings. Mater. Sci. Eng. B Solid-State Mater. Adv. Technol., 131(1-3), pp. 36-39, 2006. DOI: 10.1016/j.mseb.2006.03.017.
- [7] Pogrebnjak, A., Physical-mechanical properties of superhard nanocomposite coatings on base Zr-Ti-Si-N. Medziagotyra, 19(2), pp. 140-143, 2013. DOI: 10.5755/j01.ms.19.2.4429.
- [8] Saladukhin, I.A., Structure and hardness of quaternary TiZrSiN thin films deposited by reactive magnetron co-sputtering. Thin Solid Films, 581, pp. 25-31, 2015. DOI: 10.1016/j.tsf.2014.11.020
- [9] Šúna, J., Musil, J., Ondok, V. and Han, J.G., Enhanced hardness in sputtered Zr-Ni-N films. Surf. Coatings Technol., 200(22-23) SPEC. ISS., pp. 6293-6297, 2006. DOI: 10.1016/j.surfcoat.2005.11.042.
- [10] Kumar, M. and Mitra, R., Effect of substrate bias on microstructure and properties of Ni-TiN nanocomposite thin films deposited by reactive magnetron co-sputtering. Surf. Coatings Technol., 251, pp. 239-246, 2014. DOI: 10.1016/j.surfcoat.2014.04.032.
- [11] Chu, X., Wongb, M.S., Sprout, W.D. and Barnetta, S.A., Mechanical properties and microstructures of polycrystalline ceramic / metal superlattices : TiN / Ni and TiN / Ni0 9Cr0 . 1. 61, pp. 2-7, 1993. DOI: 10.1016/0257-8972(93)90234-F.
- [12] Zhang, S., Sun, D. and Zeng, X., Oxidation of Ni-toughened nc-TiN/a-SiN x nanocomposite thin films. J. Mater. Res., 20(10), pp. 2754-2762, 2005. DOI: 10.1557/JMR.2005.0357.
- [13] Sobol', O.V., Pogrebnjak, A.D. and Beresnev, V.M., Effect of the preparation conditions on the phase composition, structure, and mechanical characteristics of vacuum-Arc Zr-Ti-Si-N coatings. Phys. Met. Metallogr., 112(2), pp. 188-195, 2011. DOI: 10.1134/S0031918X11020268
- [14] Musil, J., Zeman, P., Baroch, P., Bohemia, W. and Republic, C., 4.13 – Hard Nanocomposite Coatings, 4(1). Elsevier, 2014.
- [15] Musil, J., Hard nanocomposite coatings: Thermal stability, oxidation resistance and toughness. Surf. Coatings Technol., 207, pp. 50-65, 2012. DOI: 10.1016/j.surfcoat.2012.05.073.
- [16] He, C., Xie, L., Zhang, J. and Ma, G., Microstructure and mechanical properties of reactive sputtered nanocrystalline Ti-Al-Ni-N thin films. Surf. Coat. Technol., 320, pp. 472-477, 2017. DOI: 10.1016/j.surfcoat.2016.11.079
- [17] Hefnawy, A., Elkhoshkhany, N. and Essam, A., Ni–TiN and Ni-Co-TiN composite coatings for corrosion protection: Fabrication and electrochemical characterization. J. Alloys Compd., 735, pp. 600-606, 2018. DOI: 10.1016/j.jallcom.2017.11.169
- [18] Feng, Q., Li, T. and Teng, H., Investigation on the corrosion and oxidation resistance of Ni-Al<sub>2</sub>O<sub>3</sub> nano-composite coatings prepared by sediment co-deposition. Surf. Coatings Technol., 202(17), pp. 4137-4144, 2008. DOI: 10.1016/j.surfcoat.2008.03.001.

**E.N. Borja-Goyeneche**, completed her BSc. degree in Aeronautical Eng. at the Universidad de San Buenaventura, Bogotá, Colombia, in 2015, and is ending her MSc. degree in Engineering Materials and Processes at the Universidad Nacional de Colombia, Bogotá, Colombia. She has worked in the area of materials with aeronautical applications, production of thin films, corrosion and wear.  
ORCID: 0000-0002-4866-4792

**J.J. Olaya-Florez**, is a full professor at the Departamento de Ingeniería y Mecatrónica of the Universidad Nacional de Colombia, Bogotá Colombia. He conducts research in the general area of development and applications of thin films deposited by plasma assisted techniques, corrosion and wear. He received his PhD in 2005 from the Universidad Nacional Autónoma de México, Mexico.  
ORCID: 0000-0002-4130-9675